Dependence of four-wave mixing line-shape on micrometric atomic vapor thickness

Li Li, Yi-Xin Lu and Yuan-Yuan Li*

Institute of Optics & Electronics, Department of Physics and Optical-electronic Engineering, Xi'an University of Arts and Science, Xi'an 710065, China

Abstract. We theoretically examine thickness and wavelength dependence line-shape of four-wave-mixing (FWM) spectroscopy in micrometric thin atomic vapors whose thickness L is assumed to be 10,30,50,80 and 100 μm respectively. It is found that a narrow centre (Dicke-narrowing) persists for all cases, while wings are broadened as the thickness of the vapor increases or the pump wavelength decreases comparing to the probe wavelength. This type of spectrum is due to the modified velocity distribution and polarization interference from different ensemble of atoms in a confined situation.

1 Introduction

Width narrowed spectral lines (Dicke-narrowing) in thin vapor cells are firstly observed in optical region by Briaudeau et al. [1]. This narrowing structure spectrum is due to the enhanced contribution of slow atoms in the thin vapor, where the duration of the atom-laser interaction governed by wall-to-wall trajectories is anisotropic [2–4]. The contribution of atoms with slow normal velocity is enhanced thanks to their longer interaction time with the laser field [2–4]. Under normal incidence irradiation, the resonance of these atoms, flying nearly parallel to the wall and yielding a stronger contribution to the signal, appears to be insensitive to the Doppler shift [2–4].

Several absorption emission cycles can take place due to the fact that the longer atom-light interaction time in a micrometric vapor compared to the excited state decay [5]. However, the optical pumping efficiency is strongly dependent on the atomic velocity

---

and only the slowest atoms may approach a steady state [5]. Thus very narrow spectra can be achieved due to atom-wall collision in such a confined atomic system [5].

Many authors have demonstrated that, the cell's thickness is the main factor which influences the shape and the magnitude of the spectra of a thin vapor column both in theory and experiment [2–4, 6]. This modification can be extended to electromagnetically induced transparency (EIT) dips [7, 8] and FWM spectroscopy [7]. In this paper, we predict FWM lines for five type vapors with a thickness of $10, 30, 50, 80$ and 100 μm respectively. Potential applications of FWM process, e.g., the measurement of atomic exited state lifetimes [9], coherent anti-stokes Raman spectroscopy (CARS) [10], generation of coherent sources in the ultraviolet (UV) and infrared radiation (IR) [11–13] and femtosecond pulse generation [14], and generation of correlated photon pairs [15, 16] can be extended to micrometric thin vapors.

We consider three typical cases of wavelength configurations [17] corresponding to different type of polarization interference [18–20], where the cases for the probe wavelength is less, equal and greater than the pump wavelength are respectively termed as mismatched case I, matched case, and mismatched case II [17, 20]. A narrow line centre persists for all lines of micrometric thin vapors, while wings are broadened as the thickness of the vapor increases or the pump wavelength decreases comparing to the probe wavelength. Very narrowing FWM lines can be achieved in experiment by using proper thin vapor cells. This type of spectrum can be demonstrated by the transient effect of confined atoms and polarization interference from different ensemble of atoms in thin vapors.

2   Theoretical model

We consider a phase-conjugated beam configuration (Fig. 1(a)) applied to a cascade three-level atomic system (Fig. 1(b)), where $|0\rangle$, $|1\rangle$ and $|2\rangle$ are the ground, the intermediate and the excited states respectively. Beam 1 represents the probe field ε_1, beams 2 and 3 propagating with a small angle difference (about 0.5°) consist of pump fields ε_2 and ε_2' respectively. Rabi frequencies g_1, g_2 and g_2' are respectively defined as $g_1 = \mu_{10}\varepsilon_1/\hbar$, $g_2 = \mu_{21}\varepsilon_2/\hbar$ and $g_2' = \mu_{21}\varepsilon_2'/\hbar$. The FWM signal can be generated and propagates almost opposite to the beam 3 if the phase-matching condition $k_F = k_1 + k_2 + k_2'$ is satisfied, where $k_i(k_i')$ is the wave vector of the field $\varepsilon_i(\varepsilon_i')$ ($i = 1, 2$).

We define

$$\Lambda_{10} = \Gamma_{10} + i(k_1\nu + \Delta_1), \quad \Lambda_{20} = \Gamma_{20} + i(k_1\nu + k_2\nu + \Delta_1 + \Delta_2)$$

as the Doppler-shifted detunings with Γ_{10} and Γ_{20} the decay rate from level $|1\rangle$ to $|0\rangle$ and the dephasing rate between level $|2\rangle$ and $|0\rangle$ respectively, $\Delta_i = \Omega_i - \omega_i$ ($i = 1, 2$) the detuning of the field $\varepsilon_i(\varepsilon_i)'$, and Ω_1 and Ω_2 the transition frequencies of $|0\rangle - |1\rangle$ and $|1\rangle - |2\rangle$ respectively. Considering that the coherence σ_{21} is much less than the coherence σ_{10} and σ_{20} in a steady state, and the factor before σ_{21} in coupling equations is the Rabi

frequency g_1 of the weak probe field $(g_1 \ll g_2(g_2'))$, we then neglect σ_{21}, and write down following coupling equations [20]

$$\partial \sigma_{10}^{(1)} / \partial t = -\Lambda_{10} \sigma_{10}^{(1)} + i g_1 \sigma_{00}^{(0)}, \tag{1}$$

$$\partial \sigma_{20}^{(2)} / \partial t = -\Lambda_{20} \sigma_{20}^{(2)} + i g_2 \sigma_{10}^{(1)}, \tag{2}$$

$$\partial \sigma_{10}^{(3)} / \partial t = -\Lambda_{10} \sigma_{10}^{(3)} + i g_2' \sigma_{20}^{(2)}. \tag{3}$$

The coupling Eqs. (1)-(3) can be solved by combining a process. One then obtains [20]

$$\sigma_{00}^{(0)} \xrightarrow{\omega_1} \sigma_{10}^{(1)} \xrightarrow{\omega_2} \sigma_{20}^{(2)} \xrightarrow{-\omega_2} \sigma_{10}^{(3)}. \tag{I}$$

$$\sigma_{10}^{(3)}(t) = -i g_1 g_2 g_2' \Big(A + B \exp(-\Lambda_{10}t) + Ct \exp(-\Lambda_{10}t) + D \exp(-\Lambda_{20}t) \Big), \tag{4}$$

where

$$A = \frac{1}{(\Lambda_{10}^2 \Lambda_{20})}, \qquad B = \frac{(2\Lambda_{10} - \Lambda_{20})}{\Lambda_{10}^2(\Lambda_{10} - \Lambda_{20})^2},$$

$$C = \frac{1}{\Lambda_{10}(\Lambda_{10} - \Lambda_{20})}, \qquad D = \frac{-1}{\Lambda_{20}(\Lambda_{20} - \Lambda_{10}^2)}.$$

To solve the coupling Eqs. (1)-(3), we assume that the initial conditions are $\sigma_{00} = 1$ and $\sigma_{i0}(t=0) = 0$ $(i=1, 2)$.

The intensity of the FWM signal can be calculated by $I_{FWM} \propto |\int_0^L P(z)dz|^2$ with $P(z)$ the local nonlinear polarization, L the thickness of the thin vapor. When considering the Doppler effects of thermal atoms, the nonlinear polarization can be expressed as

$$P(z) = N\mu_{10} \int_{-\infty}^{\infty} W(v) \sigma_{10}^{(3)}(t)dv, \tag{5}$$

where

$$W(v) = (u\sqrt{\pi})^{-1} \exp(-v^2/u^2)$$

is the Maxwell distribution with u being the probable velocity of thermal atoms, N the density of atoms, μ_{10} the dipole moment matrix element.

It is assumed that atoms get de-excited at a collision with the wall, and are in the ground states at the instant that they leave the wall after a collision, thus we take $t = z/v$ for $v > 0$ and $t = (z-L)/v$ for $v < 0$ in in Eq. (4), then into Eq. (5), and change the integrate orders of v and z, and we finally obtain [20]

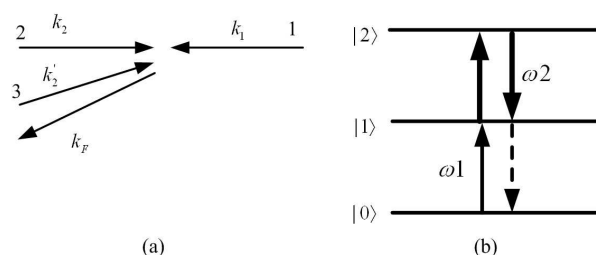$$I_{FWM} \propto |\int_{-\infty}^{+\infty} W(v)dv(F_1 + F_2 + F_3)|^2, \tag{6}$$

Figure 1: Beam configuration (a) and level diagram (b) of FWM in a cascade three-level atomic system.

where

$$F_1 = AL, \quad F_2 = \frac{B|v|}{\Lambda_{10}} + C|v|\Lambda_{10}^2 + \frac{D|v|}{\Lambda_{20}},$$
$$F_3 = \frac{-B|v|}{\Lambda_{10}} \exp\left(\frac{-\Lambda_{10}L}{|v|}\right) - \frac{C(|v| + \Lambda_{10}L)}{\Lambda_{10}^2} \exp\left(\frac{-\Lambda_{10}L}{|v|}\right) - \frac{D|v|}{\Lambda_{20}} \exp\left(\frac{-\Lambda_{20}L}{|v|}\right).$$

The modulation behavior from the thickness of the vapor is mainly dependent on F_3 in Eq.(6), in which three terms are included. The former two and the third damping terms in F_3 illustrate atom-light interaction of FWM from one-photon and two-photon processes. These two processes can be modified by the interaction time $L/|v|$ in a thin vapor and give the thickness dependence features of FWM lines in a confined atomic system.

3   Results and discussion

In numerical calculation, the wavelength of the probe field is taken to be 800nm, and the wavelength of the pump fields is selected to be 1600 nm, 800 nm and 400 nm respectively for the mismatched case I $(\lambda_1 < \lambda_2)$, the matched case $(\lambda_1 = \lambda_2)$ and the mismatched case II $(\lambda_1 > \lambda_2)$ [17,20]. We take $k_1 > 0$ and $k_2 < 0$ for our beam configuration as shown in Fig. 1(a), decay rates $\Gamma_{10} = \Gamma_{20} = 42$ MHz, and the probable velocity of atoms $u = 270$ m/s.

Thickness dependence normalized FWM lines versus the probe detuning Δ_1 for three cases of $\lambda_1 = 1600$, 800 and 400 nm are predicted in Figs. 2 (a), (b) and (c) respectively, where solid, dashed, dotted, dash dot and short dashed lines are respectively for $L = 10$, 30, 50, 80 and 100 μm respectively. Wavelength (polarization interference) dependence FWM lines for different thickness of the vapor are shown in Fig. 3, where solid, dashed and dotted lines respectively represents the mismatched case I, matched case and the mismatched case II. The signal is normalized by the maximum value of the signal for $\Delta_1 = \Delta_2 = 0$ in each case.

It can be found in Fig. 2 and Fig. 3 that a narrow line centre persists for all five type cell's and all three type wavelength configuration, while a broadening wing appears as the thickness of the cell gets greater or the pump wavelength decreases comparing to
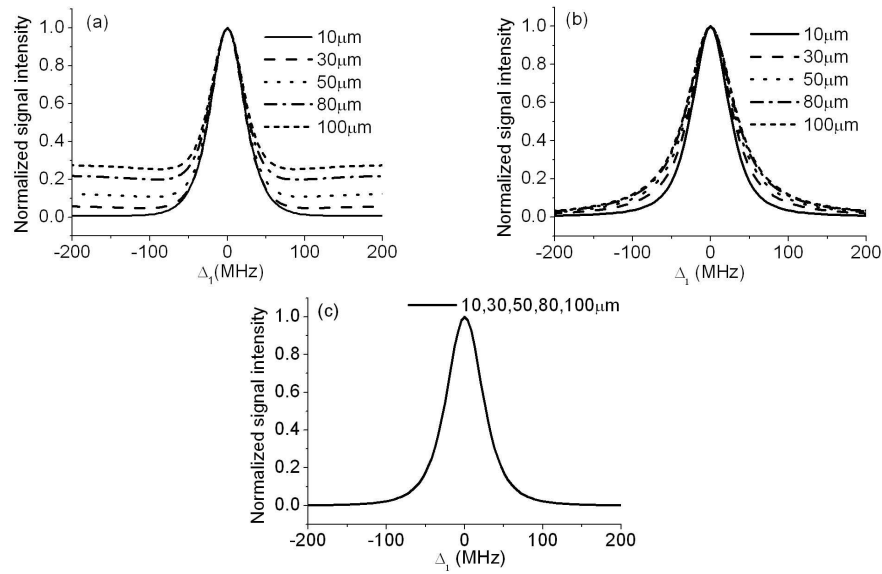
Figure 2: Normalized signals versus the probe detuning Δ_1 for $L=10$ (solid lines), 30 (dashed lines), 50 (dotted lines), 80 (dash dot lines) and 100 μm (short dashed lines), (a), (b) and (c) for $\lambda_2 = 1600$, 800 and 400 nm respectively. The signals for $\Delta_1 = \Delta_2 = 0$ is normalized to be 1 in each wavelength regime.

the probe wavelength. This type of spectrum is due to velocity distribution modified by cell's thickness and polarization interference from different ensemble of atoms in a confined situation.

The atom-laser interaction time is governed by wall-to-wall trajectories, thus the contribution of atoms with slow normal velocity is enhanced thanks to their longer interaction time with the laser field, while atoms flying nearly parallel to the wall and yielding a stronger contribution to the signal, appears to be insensitive to the Doppler shift [2–4]. Thus very narrow line centre can be achieved due to atom-wall collision in thin vapor cells [5]. As shown in Fig. 2 and Fig. 3, the FWM lines reach a minimum width value about 50 MHz for $L=10$ μm or $\lambda_2 = 400$ nm, and then a slightly broadening (e.g. from 50MHz to 60 MHz in Fig. 2(a)) as the thickness of the vapor increases for matched case and mismatched case I. A broadening wing of FWM lines is mainly from the contribution of relatively fast atoms in the thin vapor, which can be enhanced for a relatively greater thickness of the vapor or a relatively smaller pump wavelength. In a relatively greater thickness of the vapor, atoms with relatively greater velocities participate in the light-atom interaction and result in a broadening wing. This broadening can be overcome by using a very thin vapor or a proper wavelength configuration, e.g., a 10 μm vapor cell or mismatched case II, since the contribution of relatively fast atoms can be limited in the former case in a confined situation or can be wash out by polarization interference from different ensemble of atoms. Thus the width broadening induced by polarization interference can be overcome in micrometric thin cells, and Dicke-narrowing structure from an enhanced contribution of slow atoms induced by atom-wall collision in micrometric
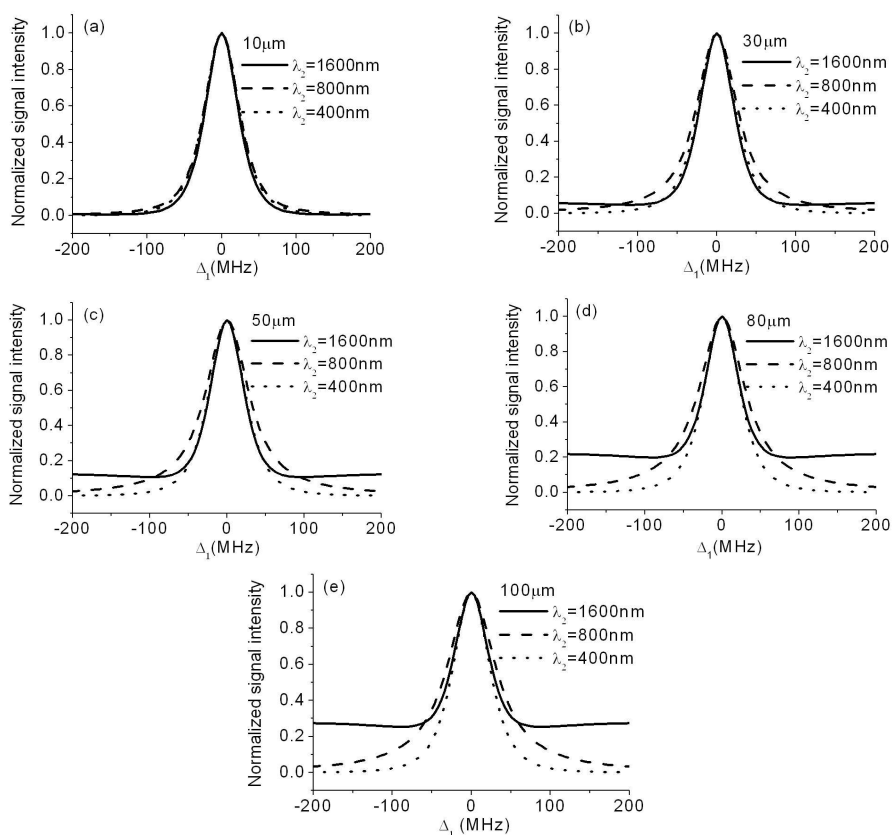
Figure 3: Normalized signals versus the probe detuning Δ_1 for $\lambda_2 = 1600$ (solid lines), 800 (dashed lines) and 400 nm (dotted lines), (a), (b), (c), (d) and (e) for $L = 10, 30, 50, 80$ and 100 μm respectively. The signals for $\Delta_1 = \Delta_2 = 0$ is normalized to be 1 in each wavelength regime.

vapors can be achieved in experiment.

4   Conclusion

In summary, we have investigated the FWM lines in 10,30,50,80 and 100 μm vapor cells for three cases of wavelength configuration: mismatched case I ($\lambda_1 < \lambda_2$), the matched case ($\lambda_1 = \lambda_2$) and mismatched case II ($\lambda_1 > \lambda_2$). It is found that FWM lines shape can be dramatically modified by the thickness of the thin vapor and the polarization interference in different wavelength configuration. A narrow line centre persists for all five type thickness and all three type wavelength configuration, while wings are broadened as the thickness of the cell increases or the pump wavelength decreases comparing to the probe wavelength. This type of spectrum is due to modified velocity distribution and polarization interference from different ensemble of atoms in the thin vapor. Thus the width broadening induced by polarization interference can be overcome in proper

micrometric thin cells, and Dicke-narrowing structure in micrometric vapors is feasible to be achieved in experiment. Potential applications in a robust experiment, such as the measurement of atomic exited state lifetimes, coherent anti-stokes Raman spectroscopy (CARS), generation of coherent sources in the ultraviolet (UV) and infrared radiation (IR) can be extended to micrometric thin vapors.

References

[1] S. Briaudeau, D. Bloch, and M. Ducloy, Europhys. Lett. 35 (1996) 337.
[2] A. Sargsyan, D. Sarkisyan, and A. Papoya, Phys. Rev. A 73 (2006) 033803.
[3] G. Dutier, A. Yarovitski, S. Saltiel, A. Papoyan, D. Sarkisyan, D. Bloch, and M. Ducloy, Europhys. Lett. 63 (2003) 35.
[4] D. Sarkisyan, T. Varzhapetyan, A. Sarkisyan, Yu. Malakyan, A. Papoyan, A. Lezama, D. Bloch, and M. Ducloy, Phys. Rev. A 69 (2004) 065802.
[5] H. Failache, L. Lenci L, A. Lezama, D. Bloch, and M. Ducloy, Phys. Rev. A 76 (2007) 053826.
[6] G. Dutier, S. Saltiel, D. Bloch, and M. Ducloy, J. Opt. Soc. Am. B 20 (2003) 793.
[7] Y. Li, J. Bai, L. Li, W. Zhang, C. Li, Z. Nie, C. Gan, and Y. Zhang, Chinese Phys. Lett. 25 (2008) 3238.
[8] Y. Li, X. Hou, J. Bai, J. Yan, C. Gan, and Y. Zhang, Chinese Phys. B 17 (2008) 2885.
[9] A. Debarre, J. L. Le Gouet, I. Lorgere, and P. Tchenio, J. Phys. B: At. Mol. Opt. Phys. 26 (1993) 3435.
[10] N. Dudovich, D. Oron, and Y. Silberberg, Nature 418 (2002) 512.
[11] U. Czarnetzki and H. F. Dobele, Phys. Rev. A 44 (1991) 7530.
[12] K. H. Hahn, D. A. King, and S. E. Harris, Phys. Rev. Lett. 65 (1990) 2777.
[13] C. Dorman and J. P. Marangos, Phys. Rev. A. 58 (1998) 4121.
[14] S. E. Harris and A. V. Sokolov, Phys. Rev. Lett. 81 (1998) 2894.
[15] V. Balic, D. A. Braje, P. Kolchin, G. Y. Yin, and S. E. Harris, Phys. Rev. Lett. 94 (2005) 183601.
[16] S. W. Du, J. M. Wen, M. H. Rubin, and G. Y. Yin, Phys. Rev. Lett. 98 (2007) 053601.
[17] J. R. Boon, E. Zekou, D. McGloin, and M. H. Dunn, Phys. Rev. A 59 (1999) 4675.
[18] Z. Zuo, J. Sun, X. Liu, L. Wu, and P. Fu, Phys. Rev. A 75 (2007) 023805.
[19] Y. Li, L. Li, J. Bai, C. Li, Y. Zhang and X. Hou, Chinese Phys. Lett. 27 (2010) 044203.
[20] Y. Li, L. Li, Y. Zhang, and S. Bi, Wavelength dependence four-wave mixing spectroscopy in a micrometric atomic vapour, Chinese Phys. B, to be published.